ELSEVIER

13 May 1994

Chemical Physics Letters 222 (1994) 224–232

CHEMICAL PHYSICS LETTERS

Femtochemistry at high pressures. Solvent effect in the gas-to-liquid transition region

Ch. Lienau [1], A.H. Zewail

Arthur Amos Noyes Laboratory of Chemical Physics [2], California Institute of Technology, Pasadena, CA 91125, USA

Received 22 March 1994

Abstract

We report new studies on the effect of solvent on the femtosecond dynamics of the dissociation and recombination of iodine in the gas-to-liquid transition region. The pressure of the solvent (helium, neon, argon and krypton) spans the range from 0 to 2500 bar, corresponding to solvent densities from the ideal gas-phase limit to the liquid-like fluid regime. The reactive cross section and the dynamics of the collision of the fragments with the solvent and with each other are discussed in relation to the solvent polarizability and the structure of the solvent cage.

1. Introduction

In this Letter, we report new studies of the solvent effect on the real-time dynamics of an elementary chemical reaction in the gas-to-liquid transition region of the solvent. The reaction is that of iodine dissociation and recombination in compressed gases; solvent densities are changed to cover the range from the ideal gas-phase limit to the liquid-like fluids. These experiments are aimed at understanding the solute–solvent dynamical interactions on the femtosecond and longer time scales. The fact that the solute (iodine) wave packet motion, under collisionless conditions, is well understood makes the following questions pertinent: How is the dynamics affected when the solute is perturbed by a monoatomic solvent under controlled densities, and how do these changes in the dynamics depend on the properties (density, polarizability, mass, size, etc.) of the solvent?

In a recent publication [1], the dissociation and recombination of iodine were probed in supercritical argon at pressures reaching 2000 bar. With femtosecond time resolution, we followed the change in the dynamics with solvent density and studied the coherent nuclear motion, the predissociation to I+I, and the recombination of dissociated iodine atoms. Within the pressure range of our experiments, the state of the solvent was gradually changed: variation of the argon pressure allowed us to study the effect of increasing the *number* of argon–iodine collisions on the dynamics as the time between collisions was brought to the time scale of the nuclear motion of the iodine molecule. Through variation of the rare-gas solvent atom, we can now examine the nature of *each* iodine–solvent collision and the dependence on the mass, the momentum and electronic polarizability of the rare-gas collision partner. In each solvent (He, Ne, Ar and Kr), experiments are performed over a wide range of pressures between 0 and 2500 bar.

[1] Deutsche Forschungsgemeinschaft Postdoctoral Fellow.

[2] Contribution No. 8933.

SSDI 0009-2614(94)00384-3

Iodine seems to be a particularly attractive model system for such a study. A wealth of spectroscopic and dynamic information is available, both in the isolated gas phase and in solutions. The potential energy curves of the isolated molecule in the ground $X0_g^+(^1\Sigma)$ and excited $B0_u^+(^3\Pi)$ state are known. Moreover, detailed spectroscopic information is also available on the dissociative and ion-pair states of iodine, which are relevant to the present study. Of particular relevance to the present work are the thorough studies by nanosecond laser flash photolysis in compressed gases by the groups of Troe [2] and van den Bergh [3]. From accurate measurements of the quantum yields for geminate recombination (at long times) they have shown the dependence of the yield on pressure and solvent, and advanced a diffusion model to account for these dependencies.

The femtosecond wave packet dynamics on the bound $B0_u^+(^3\Pi)$ state and on the $A1_u(^3\Pi)$ and $B''1_u(^1\Pi)$ have been studied under collisionless conditions [4]. The effect of one argon solvent atom (in a van der Waals complex) on electronic predissociation rates to I+I+Ar have also been investigated in the half collision [5]. For the full collision at higher pressures (up to 100 bar), our first femtosecond time-resolved experiments [6] demonstrated the effect of argon collisions on vibrational coherences of the wave packet, the collision-induced B-state predissociation, and the caging of iodine molecules excited above the B-state dissociation threshold. Molecular dynamics simulations by Wilson's group [7] have shown agreement with experiments and identified the time scale of the caging at different translational energies.

In solution, geminate recombination of dissociated iodine atoms has been the subject of numerous time-resolved studies. Following Eisenthal's pioneering work on the picosecond ground-state recovery in CCl_4 [8], theoretical and experimental studies by several groups (Adelman, Bunker, Harris, Hopkins, Hynes, Kelley, Miller, Moore, Sceats, Wilson, and others) have been made, and the progress is summarized in Harris' excellent review [9]. Basically, B-state excitation leads to a rapid electronic predissociation; recent experiments by Scherer et al. [10] found a predissociation time of 230 fs in liquid *n*-hexane, consistent with Raman [11] and femtosecond [6] results in CCl_4. The formed atomic fragments transfer their excess kinetic energy to the solvent and recombine within two picoseconds onto either the A/A′ or the ground X state. This is followed by a slower vibrational relaxation in both states, as predicted by Nesbitt and Hynes [12]. Molecules trapped on the A/A′ state undergo subsequent curve-crossing, onto the X-state surface, and A/A′-state lifetimes are found to be strongly solvent dependent, ranging from 100 ps to 10 ns [13]. The ultrafast geminate recombination dynamics, however, could not be resolved on the picosecond time scale before recent studies on the dynamics of iodine in large argon clusters [14] and cold rare-gas matrices [15] emerged.

Liu and co-workers [14] have demonstrated that after dissociation on the repulsive A state the recombination of fragment iodine atoms to form the iodine bond occurs after 600 fs as a *coherent* process in the solvent cage. The recombination, however, depends on the time scale of bond breakage. For B-state dissociation, the primary caging is not prompt and coherent as for the A-state dynamics. Thus, the time scale for solvent rearrangement relative to the dissociation time is fundamental to the nature of caging [14]. Apkarian and co-workers [15] studied the dynamics of I_2 in argon and krypton matrices and indeed observed a similar time scale as for the A-state dynamics in clusters. Furthermore, they showed manifestations for the persistence of this coherence after recombination.

In this work our focus is on the predissociation from the B state and recombination in different solvents. (Elsewhere, we will detail the dynamics following excitation to other states and energies.) In these experiments we use 60 fs laser pulses, centered at 620 nm, to excite ground state iodine atoms. A large fraction, 62%, of the excited molecules reach low vibrational levels $v'=6$–11 of the bound $B0_u^+(^3\Pi)$ state [4] (centered around $v'=8$), while 34% are placed on the weakly bound $A1_u(^3\Pi)$ state and the remainder on the dissociative $B''1_u(^1\Pi)$ state [16]. The dynamics of the prepared wave packet is then interrogated by a second 60 fs, 310 nm pulse, which can excite molecules near the outer turning point of the B state into either the $f0_g^+$ or $E0_g^+$ ion-pair states of iodine. We detect the laser-induced fluorescence as a function of the delay time between pump and probe pulses. The fluorescence is a measure of the B-state population at the probed internuclear distances. The probe can also

monitor molecules from low vibrational levels [17] of the weakly bound $A'2_u(^3\Pi)$ and $A1_u(^3\Pi)$ states by excitation into the $D'2_g$ or $\beta 1_g$ ion-pair states. Fluorescence induced by molecules in high vibrational levels on the ground state, however, could be shown to be negligible under these conditions. Thus, in our experiments, we are mainly sensitive to the coherent wave packet motion within the bound B state, the collision-induced B-state predissociation and the recombination of the dissociating atom pair followed by vibrational relaxation on the A/A′ states.

2. Experimental

The experimental setup used is similar to the one described elsewhere [18] and will only be briefly discussed here. The fs laser pulses were generated from a colliding-pulse mode-locked ring dye laser (CPM) and amplified in a four-stage, Nd:YAG-pumped dye amplifier (PDA). The amplified pulses were temporally recompressed in a double-pass, two-prism arrangement before being separated into pump and probe lasers by a 50/50 beam splitter. The probe fs laser pulse was focused into a KD*P crystal to generate the 310 nm pulse, and the fundamental was removed with a UG 11 filter. The relative timing between the two pulses was varied with a high-precision, computer-controlled actuator.

The pump arm contained two polarizers and a half-wave plate to allow variation in the angle between the polarizations of the two lasers, and this angle was kept constant at 54.7° (rotational anisotropy effects in the transients will be detailed later). The pump and probe lasers were recombined with a dichroic beam splitter and then focused slightly beyond the center of the high-pressure cell. Care was taken to prevent continuum generation within the cell. Laser-induced fluorescence was collected perpendicular to the laser propagation direction, collimated into a monochromator, and detected with a photomultiplier tube (PMT).

The high-pressure cell was constructed from stainless steel and designed to withstand pressures of up to 4000 bar. Details of the design and the precision measurements will be given in the full account of this work. Four windows, 6 mm in diameter, were centered in each of the four walls, and the cell had a total volume of 0.2 cm^3. The input window was 4.0 mm thick quartz, while the output and fluorescence-collection windows were 2.8 mm thick sapphire. Pressure in the cell was monitored with a precision strain-gauge pressure transducer. After introducing the iodine carefully, the cell was filled with the solvent gas, which was compressed to the desired pressure in an iterative process. To reach the highest pressures, the solvent was precompressed by cooling or liquefying the gas in a pressure-resistant cryotrap. The high-pressure cell showed no decrease in pressure during the course of an experiment.

Fluorescence signal from the PMT was averaged in a boxcar integrator and recorded as a function of actuator position in a computer. The transients were fitted to a sum of exponential rise and decay functions using standard software that takes into account the 60 fs pulse widths.

As mentioned before, excitation from the B state is either to the $E^3\Pi(0_g^+)$ or $f(0_g^+)$ ion-pair states. If argon or krypton is the solvent, a rapid electronic quenching [19] from the E or f to the D′ state is induced, so that the detected fluorescence comes entirely from the D′→A′ transition, which is strongly pressure dependent. The maximum of this transition is found to be shifted from 342 nm at 0 bar to 374 nm at 2000 bar argon and to 370 nm at 300 bar krypton. In the lighter rare gases this pressure-induced shift is far less pronounced (from 342 nm at 0 bar to 345 nm at 2000 bar helium and to 347.5 nm at 2080 bar neon). The shift is attributed to a solvent-induced lowering of the D′ state and is consistent with similar observations in clusters [14,20], rare-gas matrices [21] and in the liquid phase [9].

Two additional fluorescence bands were observed at 270 and 290 nm in helium and in neon even at the highest pressures. This indicates that electronic quenching of the initially excited ion-pair-state is less effective in these solvents than in argon or krypton. In argon at high pressures and in krypton at pressures above 200 bar, the 310 nm probe pulses alone gave rise to a broad fluorescence between 310 and 410 nm, the intensity of which increased strongly with pressure. In krypton at pressures above 400 bar this fluorescence became much more intense than the two-photon fluorescence induced by pump and probe lasers, so that experiments at higher krypton pressures became very difficult. This fluorescence is likely to

arise from iodine–solvent charge transfer complexes which are known to be present in polar liquids (for reviews see, e.g., ref. [22]). The results of our spectroscopic studies will be discussed in detail in the full manuscript which is now in preperation.

3. Results and discussion

The experimental transients can be characterized as follows. In all solvents and at all pressures, we observe an initial decay (Fig. 1). The decay time decreases monotonically with pressure, and, at a given pressure, decreases with solvent mass (Fig. 2). The observed decay reflects the population loss from the originally excited iodine B state due to collision-induced predissociation. At relatively high pressures, this initial decay is followed by a rise (Fig. 3) in the LIF signal. The amplitude of this rising transient relative to the initial B-state fluorescence intensity increases with pressure, and, at a given pressure, increases with solvent mass (Fig. 4). The rise time is found to decrease with increasing pressure. This rising intensity is from iodine atoms that geminately recombine on the A/A′ states; the rise time reflects the geminate recombination dynamics and the subsequent vibrational relaxation within the A/A′ state [17]. Another main characteristic of the experimental transients is the dephasing of the oscillatory wave packet motion manifested in the strong modulation present in the LIF in the absence of collisions. These different aspects of the dynamics of the iodine reac-

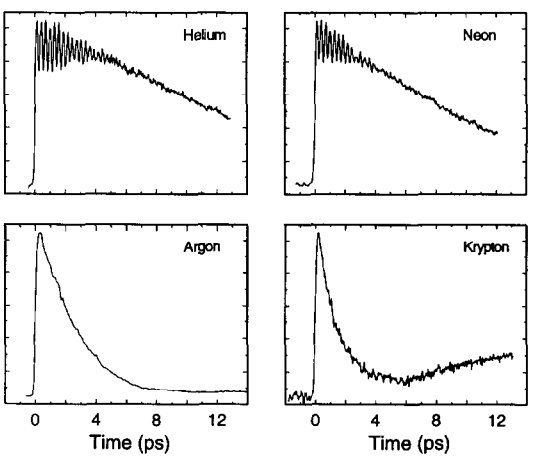

Fig. 1. Bond breakage: solvent-induced predissociation. Femtosecond transients (up to 13 ps) for iodine in supercritical rare gases (helium, neon, argon and krypton) at a temperature of 293 K and a pressure of 400 bar. LIF detection at the 'magic-angle' (54.7°) between the pump and probe pulses was used (see text). Fluorescence detection wavelength: helium and neon: 270 nm, argon: 357 nm, and krypton: 380 nm.

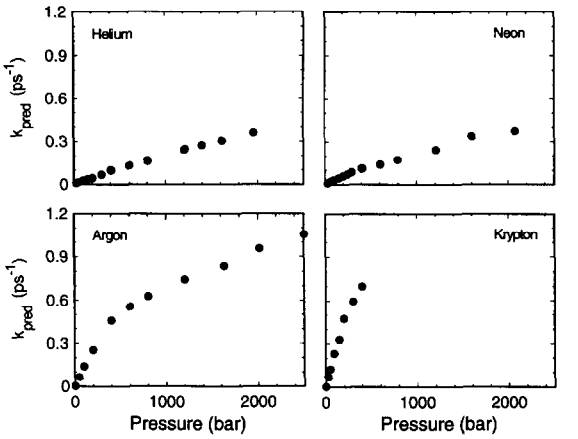

Fig. 2. Collision-induced iodine B-state predissociation rates in rare gases (helium, neon, argon and krypton) at pressures between 0 and 2500 bar and at a temperature of 293 K. Excitation is at 620 nm.

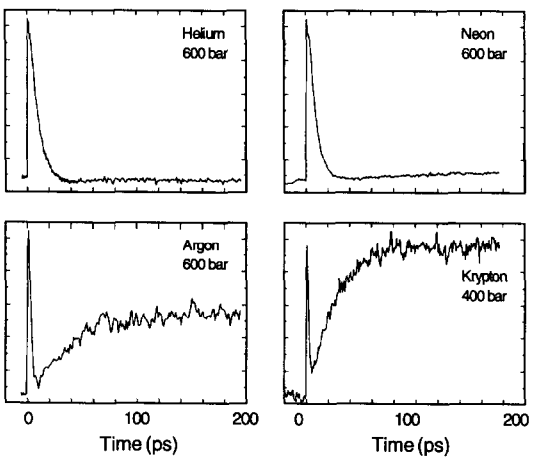

Fig. 3. Bond making by recombination: solvent-induced caging. Experimentally observed transients (up to 200 ps) for iodine in supercritical rare gases at 293 K and at pressures of 600 bar (helium, neon and argon) and 400 bar (krypton). The fast decay at early times shows the collision-induced B-state predissociation, while the build-up at long times reflects the geminate recombination and subsequent vibrational relaxation on the A/A′ state surface. Fluorescence detection wavelength: He: 344 nm; Ne: 346 nm, Ar: 362 nm and Kr: 380 nm.

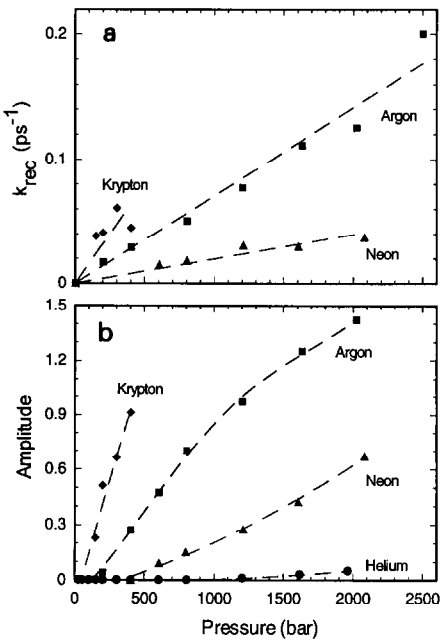

Fig. 4. Bond making through recombination. (a) Recombination rate k_{rec} for iodine in neon, argon and krypton as a function of pressure. These rise times reflect the recombination dynamics of iodine atoms and the sub-sequent vibrational relaxation dynamics within the A/A′ states. Experimental conditions, see Fig. 1. (b) Amplitude of the LIF intensity at long times ($t = 170$ ps), relative to the initial B state signal (recombination amplitude a) in helium, neon, argon and krypton for pressures between 0 and 2500 bar. The amplitudes reflect the probability for geminate recombination on the A/A′ state.

tion in rare-gas solvents will be addressed separately in the next sections.

3.1. Coherent wave packet dynamics

In our previous study in supercritical argon we reported the persistence of coherent wave packet motion in the B state for more than 1.5 ps ($\approx$ five vibrational periods) at pressures as high as 800 bar. A decrease in modulation depth with increasing pressure was noted; at pressures above 1200 bar the oscillatory modulation could no longer be resolved. In helium and neon, the coherent vibrational motion on the B state persists even longer, for more than 3 ps (or more than 10 vibrational periods) at the highest pressures (2000 bar), see Fig. 1. The modulation depth within the first 10 vibrational periods changes only slightly with pressure and is similar to the modulation depth observed in the absence of collisions. The pronounced recurrence of the signal modulation, which is present in the 0 bar transient at delay times of about 9 ps, is absent at high pressures (more than 100 bar). This indicates that it is not possible to describe the loss of coherence by the usual single exponential dephasing rate. Similar studies in argon also indicate the absence of the recurrences, consistent with previous work [6]. The damping of the oscillatory modulation in this case reflects population loss in the B state due to collision-induced predissociation. Similar to argon, an increase in the frequency of the oscillatory modulation is noted in helium, where solvent-induced changes of the B-potential energy surface are expected to be relatively small. These changes have been discussed in ref. [1] in relation to the force imposed by the solvent.

In krypton, the oscillatory modulation is efficiently damped at higher pressures. Coherences can only be detected at pressures of less than 150 bar. We note that this does not correspond to a very rapid exponential damping of the modulation. At a pressure of 100 bar krypton, more than ten oscillatory cycles can be resolved, though with a significantly reduced modulation depth. These findings will be quantified when the transients are analyzed for all densities. Comparisons to molecular dynamics simulations are in progress.

3.2. Bond breakage: solvent-induced predissociation

The collisions of iodine with the solvent cause not only a dephasing of the B-state wave packet but also induce an electronic predissociation (quenching) to form two ground state iodine atoms. This latter process occurs via a (dipole-induced) electronic curve crossing into a repulsive potential, either the $a1_g(^3\Pi)$ or the $a'0_g^+(^3\Sigma^-)$ state. (Both states cross the B potential at low energies; $a1_g$ crosses near the outer turning point of $v' = 1$ and $a'0_g^+$ crosses near $v' = 5$ (see discussion in ref. [10]). At very low foreign gas pressures ($< 10^{-3}$ bar) the predissociation rate has been related to the quenching probability p_{pred} per collision and the collision frequency. A quenching cross section, σ_{pred}, is defined as the product of p_{pred} and the cross section of the collision pair [23]. Predissociation rates are then given by

$$k_{\text{pred}} = \sigma_{\text{pred}} \bar{v} N_A \rho \,, \quad (1)$$

where $\bar{v}$ is the mean thermal velocity (m/s) of the collision pair, N_A is Avogadro's number and ρ the solvent density (mol/m^3). At a pressure of 4×10^{-5} bar and at room temperature the quenching cross sections have been measured by Capelle and Broida [24] to be: He: 1.4 Å^2, Ne: 4.4 Å^2, Ar: 17.6 Å^2, Kr: 35.8 Å^2, for excitation at 623.4 nm, and He: 1.1 Å^2, Ne: 2.6 Å^2, Ar: 16.0 Å^2, Kr: 30.5 Å^2, for excitation at 607.1 nm.

It is of particular interest to know if this concept of isolated binary collisions with a mean probability for reaction per collision still holds in the limit of very high pressures, especially as we reach the liquid-like densities. The densities of our study here are seven orders of magnitude higher than those of the early work by Capelle and Broida.

Experimentally, we observe an increase in predissociation rates with pressure in all solvents (see Fig. 2). At a given pressure, B-state decays are fastest in the heaviest rare gas studied, krypton. As a function of pressure the decay rates in krypton varies from 15 ps at 25 bar to 1.4 ps at 400 bar. A similar behavior with slightly slower rates is observed in argon, where the predissociation rates increase monotonically with pressure from 16 ps at 49 bar to 0.9 ps at 2500 bar. Relatively longer B-state lifetimes are observed in helium and neon. At a given pressure, decay rates in neon are only slightly faster than in helium, but distinctly different from those in the heavier rare gases (Fig. 2). We note a slight nonexponentiality in the fluorescence decays at early times in helium and neon. Consequently, the transient signals had to be analyzed in terms of a sum of two exponentials. The second rate constant is approximately three times faster then the predissociation rate. The amplitude of the second exponential is less than 60% of the predissociation component, and decreases to zero as the pressure is increased.

The effect of the solvent and the pressure on the collision-induced B-state predissociation is shown in Fig. 2. The predissociation rate does not increase linearly with the pressure, especially in argon and krypton. We find however a linear correlation between the predissociation rate and the (macroscopic) solvent density ρ in all four rare gases (slight deviations at the highest pressures in helium, neon and argon are noted). From a straight-line fit between k_{pred} and the solvent density ρ one obtains a quenching cross section for the different rare gases: He: 1.0 Å^2, Ne: 2.2 Å^2, Ar: 11.1 Å^2, Kr: 21.4 Å^2. The reaction cross section per collision increases drastically with increasing size of the solvent atom. In fact, through the use of simple Lennard-Jones diameters, we estimate the mean reaction probability per collision p_{pred} as: He: 0.02, Ne: 0.05, Ar: 0.20, Kr: 0.37.

The surprising similarity between our results at liquid-like densities and those from the study by Capelle and Broida at a pressure of 4×10^{-5} bar indicate that the physical mechanism which is causing the predissociation remains unaffected in spite of the drastic change in solvent density. *Binary collisions* are seemingly the key to the bond breaking dynamics even though the solvent 'packing fraction' (24% in helium and 38.5% in argon at $p=2000$ bar) is similar to the one in liquid solvents. This indicates that a short-range interaction causes the actual coupling between the bound and the repulsive state and that the actual dissociation of the molecule occurs only when iodine and the solvent atom are at very short distances. (It is interesting to note, that in the experiments on I_2X (X – rare-gas atom) van der Waals complexes [5], the repulsive length parameter was found to be 0.8 Å.) Up to rare-gas pressures of 1000 bar, many-body interactions are seemingly of less importance for the dissociation mechanism. Therefore, theoretical models which describe the predissociation probability in a single binary collision should be applicable even in very high pressure supercritical solvents, at least for this case.

Changing the solvent atom changes the nature of each particular iodine–solvent collision, i.e. the strength of the induced dipole–induced dipole interaction (which depends on the polarizability of the solvent) and the time scale of the collision (which depends on the relative velocity, and thus on the reduced mass of the collision pair). A theoretical model that describes this parametric dependence of the predissociation probability per collision on the macroscopic properties has been discussed by Selwyn and Steinfeld [25] in order to predict the solvent effect on the predissociation rates. From a Fermi Golden Rule treatment of the coupling, the quenching efficiency dependence on the solvent properties is expressed as

$$\sigma_{\text{pred}} \propto \frac{I\alpha\mu^{1/2}}{R_c^3}, \qquad (2)$$

where α is the polarizability and I the ionization energy of the solvent. The reduced mass is μ and R_c is the (hard-sphere) radius of the collision pair. For all solvents, we have plotted σ_{pred} versus the solvent parameters (as in Eq.(2)) and found a high degree of correlation with our experimental results. In other words, both the change in the polarizability and the kinematics of the solvent are accounted for. In one full account, we will attempt closer microscopic examination from knowledge of the radial distribution function and molecular dynamics.

3.3. Bond making: the solvent cage

We typically observe in all solvents (except helium) the recovery of the signal following the intial decay (see Fig. 3). The build up signal persists (or increases slightly) for at least one nanosecond. Elsewhere [17], through the use of variable wavelength probe pulses, we show that this recovery reflects the geminate recombination of a dissociating iodine atom pair onto the A/A′ states followed by subsequent vibrational relaxation within these states. As mentioned above, the probe wavelength of 310 nm is not sensitive to probing the recombination dynamics onto the ground X state. At high pressures, evidence was found for two recombination channels: an 'in-cage' primary recombination which occurs within the first few picoseconds after dissociation, and a slower secondary diffusive recombination of iodine atoms which takes place after the I atoms leave the initial solvent cage and diffuse back to form molecular iodine. Here, we focus attention on the study of the pressure and solvent dependences of the *probability* for this geminate recombination and the associated *dynamics*.

In helium, all transients (on a time scale of 0 to 200 ps) decay monotonically at pressures below 1200 bar. At higher pressures, we noticed a slight increase in the signal at long delay times; the recovery signal amplitude, however, is very low. In neon, which basically shows the same coherent and predissociation dynamics characteristic as of helium, the B-state decay is followed by a recombination rise. This rise is of the form $a\{1-\exp[-(t-t_0)/\tau_{\text{rise}}]\}$, $t_0>0$, at all pressures above 400 bar. The 'recombination amplitude' a of this rise (relative to the maximum of the B-state signal at early times, which has been normalized to unity) increases with pressure and reaches a value of 0.5 at the highest pressure of 2080 bar. The rise time, τ_{rise}, which reflects the time scale of the geminate recombination and the subsequent vibrational relaxation within the A/A′ state, decreases as the pressure increases: from 70 ps at 600 bar to about 27 ps at 2080 bar. In argon, we observe the recovery at pressures al low as 200 bar. Again, the recombination amplitude increases drastically with pressure (to 1.42 at 2020 bar), and τ_{rise} decreases to less than 10 ps. A non-exponential behavior is found at the highest pressure, and this behavior indicates the presence of two recombination channels: direct and diffusive [17]. The onset of geminate recombination is shifted to an even lower pressure value (less than 150 bar) in krypton. At a krypton pressure of 400 bar, the recombination amplitude is close to unity. As mentioned earlier, experiments could not so far be performed in Kr above 400 bar.

For the caging dynamics, we now consider the change of τ_{rise} with the density of the solvent and the asymptotic values of the yield of recombination. Under the assumption of pressure and solvent independent B- and A/A′-state absorption cross sections at 310 nm, the observed signals at 310 nm are directly proportional to the quantum yield for geminate recombination onto the A/A′ state. The assumption seems reasonable as an analysis of experimental and calculated absorption spectra shows that a wavelength of 310 nm is close to the absorption maximum in each state [17]. Neglecting a possible solvent and pressure dependence of the branching ratio for caging onto the X and A/A′ state, the recombination amplitudes are proportional to the total quantum yield for geminate recombination, which, in krypton, have been obtained before from nanosecond experiments in the groups of Troe [26] and van den Bergh [3]. Using a value for the total quantum yield of $\phi_{\text{rec}}(\text{Kr, 400 bar})=0.4$, we can estimate total quantum yield for geminate recombination as

$$\phi_{\text{rec}} = \frac{a(p)}{a(\text{Kr, 400 bar})}\,\phi_{\text{rec}}(\text{Kr, 400 bar})\,. \qquad (3)$$

This analysis indicates that in high-pressure argon at

2000 bar, more than 60% of the dissociating iodine atoms recombine geminately. With this in mind, we now compare our results to simple theoretical models for geminate recombination in an attempt to understand the origin of the strong solvent effect on the observed relative quantum yields.

Otto, Schroeder and Troe [27], have provided a description of the recombination process within the framework of a diffusion model. The process is separated into two parts: (a) the initial separation of the two iodine atoms under the influence of their repulsive interaction and the viscous drag of the solvent. In this step the excess energy of the dissociating atoms is dissipated into the solvent. The final separation distance r_0 is assumed to be identical for all molecules; (b) starting at this internuclear separation r_0, all iodine atoms undergo a random diffusive motion through the solvent. Every time the separation between the iodine atoms reaches a certain critical value R_c, the encounter radius, this 'encounter pair' decides whether to recombine (with a given probability p_{rec}) or to diffuse apart and continue their random motion. The critical parameter in the model is the probability p_{rec} for recombination of the encounter pair, which is given by the following expression:

$$p_{rec} = \frac{k_{rec}^{g}}{k_{rec}^{g} + 4\pi R_c N_A D}, \tag{4}$$

The value of p_{rec} describes the relative importance of the probability for collisional stabilization ($I+I+X \rightarrow I_2^* + X$) versus diffusional separation of the encounter pair. The constant k_{rec}^{g} (not to be confused with k_{rec}) is taken as the product of the limiting third-order rate coefficient for the non-geminate recombination of iodine at low pressures [26] and the solvent concentration: $d[I_2^*]/dt = k[I]^2[X] = k_{rec}^{g}[I]^2$. The diffusion coefficient for iodine atoms is denoted by D. The probability p_{rec} increases towards unity with increasing pressure since the solvent concentration increases and k_{rec}^{g} follows; the diffusion coefficient is inversely proportional to the density. In contrast, in the low-pressure limit $k_{rec}^{g} \rightarrow 0$ and p_{rec} goes to zero. Note that for a motion of about 5 Å and $D = 10^{-4}$ cm^2/s (e.g. in argon at 1600 bar) the time scale is about 25 ps. The total quantum yield for geminate recombination is then obtained [28],

$$\phi_{rec} = \frac{R_c}{r_0} p_{rec}, \tag{5}$$

where the factor R_c/r_0 is dependent on the initial separation of the dissociating iodine atoms and decreases to unity in the limit of high pressures. As an example we consider the case of argon at 1600 bar: $R_c = 5.5$ Å, $r_0 = 7$ Å and $p_{rec} = 0.6$; thus $\phi_{rec} = 0.5$.

Fig. 5 shows the behavior of the yield with pressures, together with the theoretical results. Our experimental estimates of ϕ_{rec} are in reasonable agreement with the predictions of the model. This supports the importance of the probability for 'in-cage' collisional stabilization of the newly formed iodine molecule (or 'cage capture') in competition to penetration of the first solvent shell ('cage break-out'). At very high pressures (or in the limiting case of iodine imprisoned in large argon clusters or matrices) this probability is close to unity, and the dynamics is entirely dominated by the ultrafast recombination within the (rigid) solvent cage. As we lower the pressure of the solvent, this probability gradually decreases and a finite fraction of the atoms can leave the solvent cage and start a diffusive motion throughout the solvent. At high pressures in argon (1600 and 2000 bar), a pronounced bi-exponentially of the recombination dynamics is observed: a large fraction of atoms recombines within a few picoseconds, while

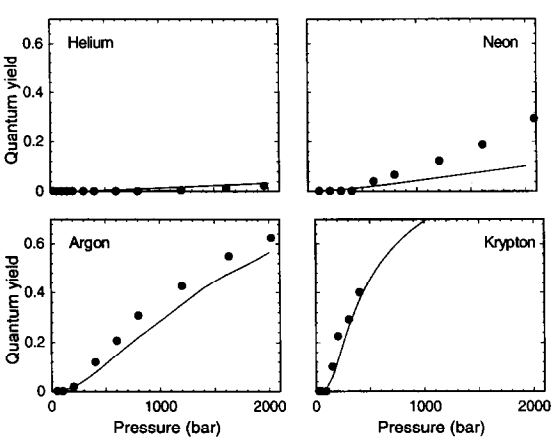

Fig. 5. Comparison of experimentally determined quantum yields for geminate recombination with theoretical values from the diffusion-based model discussed in text. Quantum yields have been obtained by normalization of the recombination amplitude a to the known experimental value for the caging yield in krypton at 400 bar of $\phi_{rec} = 0.4$ (Eq. (3)); see text.

others undergo ('secondary') recombination processes, which occur on a significantly longer time scale. A further decrease in p_{rec} (as the pressure is lowered), increases the fraction of atoms which leave the solvent cage and increases the importance of diffusive recombination. At the lowest pressures in our study, this probability tends towards zero, so that the motion of the iodine atoms is dictated by random diffusion through the solvent.

At a given pressure, a change of the solvent molecule corresponds to a change in the probability for cage capture versus cage break-out which relate to the rigidity of the first solvent shell. The change in this probability can be modeled by the decrease in diffusion coefficient and the increase in efficiency for collisional stabilization of the iodine atom pair with increasing rare-gas atom size. As for the rise time in different solvents and at different densities (Fig. 4), we are carefully examining the vibrational-to-translational energy transfer processes in the spirit of the work by Nesbitt and Hynes and with the help of molecular dynamics.

This approach of studying real-time molecular reaction dynamics systematically from the gas to the liquid phase promises several new directions for examining solvation on the time scale of the nuclear motion. Other systems are currently under investigation, and the full account of this work will be published in a series of papers.

Acknowledgement

This work was supported by the National Science Foundation. ChL gratefully acknowledges a postdoctoral fellowship by the Deutsche Forschungsgemeinschaft. We wish to thank Mr. Christopher Hyland for his help and discussions throughout this work.

References

[1] Ch. Lienau, J.C. Williamson and A.H. Zewail, Chem. Phys. Letters 213 (1993) 289.
[2] J. Troe, J. Phys. Chem. 90 (1986) 357;
J. Schroeder and J. Troe, Ann. Rev. Phys. Chem. 38 (1987) 163, and references therein.
[3] J.C. Dutoit, J.-M. Zellweger and H. van den Bergh, J. Chem. Phys. 78 (1983) 1825, and references therein.
[4] R.M. Bowman, M. Dantus and A.H. Zewail, Chem. Phys. Letters 161 (1989) 297;
M. Gruebele and A.H. Zewail, J. Chem. Phys. 98 (1993) 894.
[5] M. Gutmann, D.M. Willberg and A.H. Zewail, J. Chem. Phys. 97 (1992) 8037, 8048.
[6] A.H. Zewail, M. Dantus, R.M. Bowman and A. Mokthari, J. Photochem. Photobiol. A 62 (1992) 301.
[7] Y. Yan, R.M. Whitnell, K.R. Wilson and A.H. Zewail, Chem. Phys. Letters 193 (1992) 402.
[8] T.J. Chuang, G.W. Hoffman and K.B. Eisenthal, Chem. Phys. Letters 25 (1974) 201.
[9] A.L. Harris, J.K. Brown and C.B. Harris, Ann. Rev. Phys. Chem. 39 (1988) 341.
[10] N.F. Scherer, D.M. Jonas and G.R. Fleming, J. Chem. Phys. 99 (1993) 153.
[11] R.J. Sension and H.L. Strauss, J. Chem. Phys. 85 (1986) 3791.
[12] D.J. Nesbitt and J.T. Hynes, J. Chem. Phys. 76 (1982) 6002; 77 (1982) 2130.
[13] M.E. Paige and C.B. Harris, J. Chem. Phys. 93 (1990) 1481.
[14] E.D. Potter, Q. Liu and A.H. Zewail, Chem. Phys. Letters 200 (1992) 605;
Q. Liu, J.-K. Wang and A.H. Zewail, Nature 364 (1993) 427.
[15] R. Zadoyan, Z. Li, P. Ashjian, C.C. Martens and V.A. Apkarian, Chem. Phys. Letters 218 (1994) 504.
[16] J. Tellinghuisen, J. Chem. Phys. 58 (1973) 2821.
[17] A. Materny, Ch. Lienau and A.H. Zewail, to be published.
[18] M.J. Rosker, M. Dantus and A.H. Zewail, J. Chem. Phys. 89 (1988) 6113.
[19] A.L. Guy, K.S. Viswanathan, A. Sur and J. Tellinghuisen, Chem. Phys. Letters 73 (1980) 582.
[20] S. Fei, X. Zheng, M.C. Heaven and J. Tellinghuisen, J. Chem. Phys. 97 (1992) 6057.
[21] M. Macler and M.C. Heaven, Chem. Phys. 151 (1991) 219.
[22] M. Tamres and J. Yarwood, in: Spectroscopy and structure of molecular complexes, ed. J. Yarwood (Plenum Press, New York, 1973);
M. Tamres and R.L. Strong, in: Molecular association, Vol. 2, ed. R. Foster (Academic Press, New York, 1979) ch. 5.
[23] J.I. Steinfeld, Accounts Chem. Res. 3 (1970) 313.
[24] G.A. Capelle and H.P. Broida, J. Chem. Phys. 58 (1973) 4212.
[25] J.E. Selwyn and J.I. Steinfeld, Chem. Phys. Letters 4 (1969) 217.
[26] H. Hippler, K. Luther and J. Troe, Ber. Bunsenges. Physik. Chem. 77 (1973) 1104.
[27] B. Otto, J. Schroeder and J. Troe, J. Chem. Phys. 81 (1984) 202.
[28] R.M. Noyes, Z. Elektrochem. 64 (1960) 153; Progr. React. Kinetics 1 (1961) 131.